



# Push–pull triphenylamine based chromophores as photosensitizers and electron donors for molecular solar cells



Ana Aljarilla<sup>a</sup>, Cristina Herrero-Ponce<sup>b</sup>, Pedro Atienzar<sup>b</sup>, Susana Arrechea<sup>a</sup>, Pilar de la Cruz<sup>a</sup>, Fernando Langa<sup>a,\*</sup>, Hermenegildo García<sup>b,\*</sup>

<sup>a</sup> Instituto de Nanociencia, Nanotecnología y Materiales Moleculares (INAMOL), Univ. de Castilla-La Mancha, 45071 Toledo, Spain

<sup>b</sup> Instituto Universitario de Tecnología Química CSIC-UPV, Univ. Politécnica de Valencia, 46022 Valencia, Spain

## ARTICLE INFO

### Article history:

Received 15 April 2013

Received in revised form 28 May 2013

Accepted 31 May 2013

Available online 21 June 2013

### Keywords:

Triphenylamine

Methylenethiazole

Push–pull chromophores

Bulk heterojunction solar cells

## ABSTRACT

A series of push–pull chromophores (**1–6**) comprising triphenylamine as donor and methylenethiazole, bearing electron-withdrawing groups in the 2' position, as terminal acceptor groups have been developed. The resulting dyes were characterized by UV–vis and fluorescence spectroscopies, cyclic and OSWV voltammetries and thermal analysis. The low energy absorption band of these oligomers was located at 583–705 nm in solution. A significant positive solvatochromism, with excellent correlation with the Kamlet–Taft constant, was found confirming the charge transfer character of this band. Theoretical studies reveal a partial quinoid character in these compounds and a reduced band gap HOMO–LUMO energies of **1–6** derived from electrochemical and optical measurements were found to be suitable for their use as donor materials in combination with PCBM as acceptor in planar heterojunction solar cells. The studied devices, based on stacked cells connected electrically, incorporating these low band gap chromophores exhibited reasonable conversion efficiencies of up to 0.91% under air mass (AM) 1.5G illumination.

© 2013 Elsevier Ltd. All rights reserved.

## 1. Introduction

Organic photovoltaic cells (OPVs)<sup>1</sup> offer the advantage, with respect to analogous devices based on inorganic semiconductors, of the possibility to apply molecular design and organic synthesis to prepare a wide array of molecules having the same core structure but different substituents.<sup>2</sup> In this way the energy levels and the absorption spectra of the organic molecules can be finely tuned to maximise the efficiency of the devices.<sup>3</sup> Nowadays, small molecular semiconductors for OPV are attracting considerable attention, due to their well defined molecular structure, definite molecular weight and high purity without batch to batch variations.<sup>4</sup> Organic solar cells with an overall efficiency of 12% have been prepared with this type of molecules and C<sub>60</sub> as acceptor,<sup>5</sup> although efficiencies around 1% are not uncommon for these types of cells.<sup>6</sup>

In the area of OPVs there is much current interest in studying the performance of highly dipolar donor–acceptor (D–A) substituted  $\pi$  systems (called push–pull structures) as they can maximize the efficiency of the cell due to the combination of a high molar absorptivity with a low band gap allowing an efficient

intramolecular charge transfer (ICT). The flexibility in the design and synthesis of push–pull molecules allows exploring the performance of related analogues with the aim of rationalizing the parameters that affect the efficiency of organic solar cells based on these types of molecules.

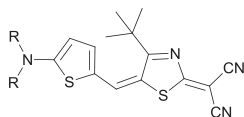
Recently it has been shown that push–pull systems can self-assemble into centrosymmetric dimers cancelling molecular dipolar moments in solid materials and the supramolecular systems demonstrating that highly dipolar D–A dyes are applicable as p-type hole conductors in bulk heterojunction (BHJ) solar cells, overcoming a serious restriction in the design of small molecules for OPV.<sup>7</sup>

Push–pull molecules having triphenylamine (TPA) have shown great potential in the field of molecular photovoltaic devices<sup>8</sup> as electron donor moiety,<sup>9</sup> stabilizing the separated hole generated from the exciton and improving hole-transport.<sup>10</sup>

Methylenethiazole moiety bearing electron-withdrawing groups in the 2'-position are excellent acceptors. Push–pull chromophores with this moiety show clear evidence for the formation of centro-symmetric dimers in concentrated solution. Self-assembly has also been found in the solid state for dicyanomethylenethiazole merocyanines.<sup>11</sup> This kind of push–pull systems gives rise to broad absorption bands, assigned to the intramolecular charge transfer (ICT), and have been used in non linear optics<sup>12</sup> as well as dyes in bulk heterojunction (BHJ) solar cells.<sup>7</sup>

\* Corresponding authors. Tel./fax: +34 925 268 43 (F.L.); tel./fax: +34 963 877 000 (H.G.); e-mail addresses: [Fernando.Langa@uclm.es](mailto:Fernando.Langa@uclm.es) (F. Langa), [hgarcia@qim.upv.es](mailto:hgarcia@qim.upv.es) (H. García).

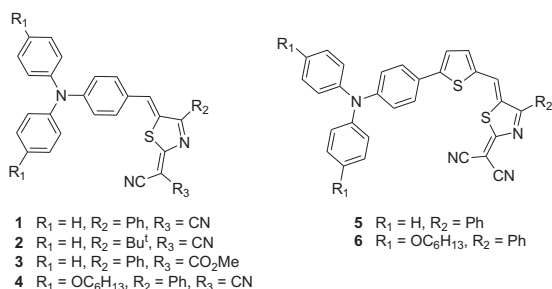
Solar cells prepared with dye HB238 (Chart 1) and phenyl-C<sub>61</sub>butyrate methyl ester (PCBM) reached an efficiency of 1.1%; spin-coated films of this dye showed a hole mobility of  $4 \times 10^{-4} \text{ cm}^2 \text{ V}^{-1} \text{ s}^{-1}$  indicating that charge transport properties are not necessarily impaired by large ground-state dipole moments of monomeric molecules.<sup>7</sup>



HB238

Chart 1. Structure of dye HB238.

Herein, we have prepared a series of push–pull chromophores (**1–6** in Chart 2) based on TPA units as donor and methylenethiazole with electron withdrawing substituents (cyano and/or carboxymethyl ester) as acceptor units showing panchromatic absorption, extending from the UV to the near-infrared region, and a narrow HOMO–LUMO gap.<sup>13</sup> Finally, using PCBM as *n*-type component and chromophores **1–6** as *p*-type semiconducting elements, we have also prepared a series of solution-processed small molecule organic solar cells (SMOSC), allowing us to draw conclusions about the properties of these chromophores.



- 1 R<sub>1</sub> = H, R<sub>2</sub> = Ph, R<sub>3</sub> = CN  
 2 R<sub>1</sub> = H, R<sub>2</sub> = Bu<sup>t</sup>, R<sub>3</sub> = CN  
 3 R<sub>1</sub> = H, R<sub>2</sub> = Ph, R<sub>3</sub> = CO<sub>2</sub>Me  
 4 R<sub>1</sub> = OC<sub>6</sub>H<sub>13</sub>, R<sub>2</sub> = Ph, R<sub>3</sub> = CN

- 5 R<sub>1</sub> = H, R<sub>2</sub> = Ph  
 6 R<sub>1</sub> = OC<sub>6</sub>H<sub>13</sub>, R<sub>2</sub> = Ph

Chart 2. New Push-Pull chromophores (**1–6**).

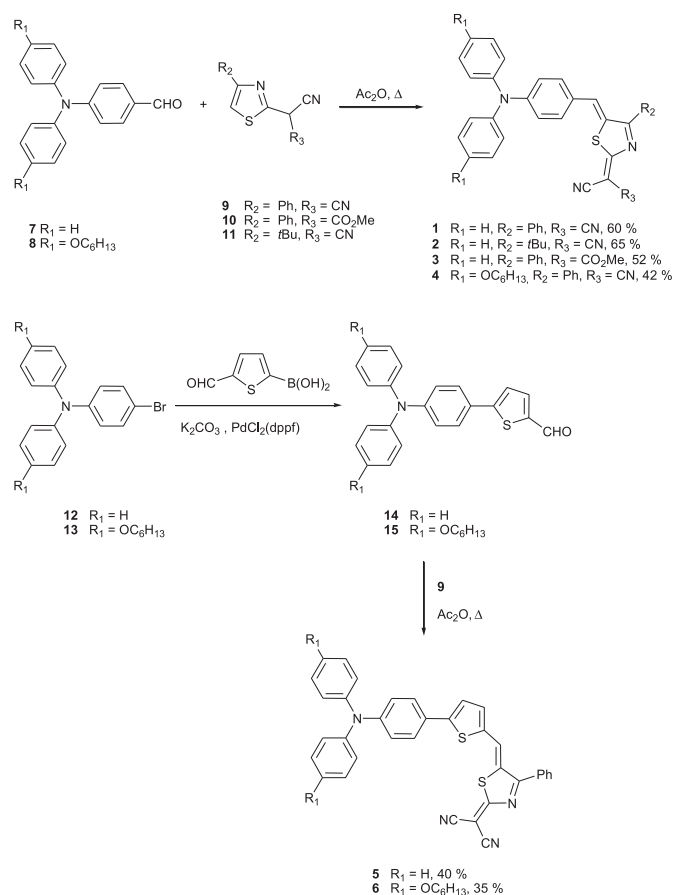
## 2. Results and discussion

### 2.1. Synthesis

The synthesis of the target compounds **1–6** is shown in Scheme 1. Chromophores **1–4** were prepared by acetic anhydride mediated condensation reaction of thiazoles **9–11**<sup>7,12,13</sup> with the corresponding aldehyde **7** or **8**.<sup>14</sup> After purification through column chromatography on silica gel, compounds **1–4** were obtained in 42–65% yield. For the synthesis of **5** and **6**, intermediate aldehydes **14**<sup>15</sup> and **15** were initially prepared in 77 and 75% yield, respectively, by Suzuki coupling of bromoanilines **12** and **13**<sup>16</sup> and 5-formyl-2-thienyl boronic acid; finally, condensation of **14** and **15** with thiazole **9** afforded **5** and **6** in 40 and 35%, respectively as dark blue solids; a single isomer (*Z*) was obtained in all cases, in concordance with the published results for similar systems.<sup>12a</sup>

All compounds were satisfactorily characterized by <sup>1</sup>H and <sup>13</sup>C NMR, FT-IR and MALDI-MS spectrometry (see the Experimental section and the Supporting data for synthetic details and full analytical and spectroscopic characterization).

The thermal stabilities of compounds **1–6** were evaluated by thermogravimetric analysis (TGA) under nitrogen, with a heating rate of 10 °C/min. The decomposition temperatures (Td) were estimated from the TGA plot as the temperature of the intercept of the leading edge of the weight loss curve. Compounds **1–6** display

Scheme 1. Synthetic route to chromophores **1–6**.

excellent thermal stability up to 300 °C with Td higher than 314 °C (Figure S15) that are in principle satisfactory for application in photovoltaic devices.

### 2.2. Optical and electrochemical properties

The optical and electrochemical properties of **1–6** have been analysed by UV–vis absorption and fluorescence emission spectroscopies; the electrochemical properties were measured by means of Cyclic (CV) and Osteryoung (OSWV) voltammetries, performed in *o*-dichlorobenzene (ODCB)-acetonitrile (5:1) solutions in the presence of tetrabutylammonium perchlorate (0.1 M) as supporting electrolyte. The corresponding results are listed in Table 1.

Table 1

Data of UV–vis and Fluorescence Emission spectroscopies<sup>a</sup> and OSWV<sup>b</sup> for compounds **1–6**

	$\lambda_{\text{max}}$ (nm)	$\log(\epsilon)$	$\lambda_{\text{em}}$ (nm) <sup>c</sup>	$E_{\text{red}}^1$ (V) <sup>d</sup>	$E_{\text{ox}}^1$ (V)	$\Delta E$ (eV) <sup>e</sup>
<b>1</b>	624	4.71	746	−0.94	0.50	1.44
<b>2</b>	583	4.73	721	−1.04	0.67	1.71
<b>3</b>	603	4.70	719	−1.01	0.60	1.61
<b>4</b>	641	4.61	776	−0.98	0.47	1.45
<b>5</b>	656	4.83	814	−0.81	0.51	1.32
<b>6</b>	705	4.51	>900	−0.83	0.27	1.10

<sup>a</sup>  $10^{-5}$  M, in dichloromethane.

<sup>b</sup>  $10^{-3}$  M in ODCB-acetonitrile (5:1) versus  $F_c/F_c^+$ , glassy carbon, Pt counter electrode, 20 °C, 0.1 M Bu<sub>4</sub>NClO<sub>4</sub>, scan rate=100 mV s<sup>−1</sup>.

<sup>c</sup>  $\lambda_{\text{exc}} = \lambda_{\text{max}}$  of each compound.

<sup>d</sup> Non-reversible processes.

<sup>e</sup> Estimated from the difference between  $E_{\text{ox}}^1$  and  $E_{\text{red}}^1$ .

The UV–vis absorption spectra of compounds **1–4** (Table 1, Figure S16), exhibit an intense absorption band in the visible region with maxima at 624 nm ( $\log \epsilon=4.71$ ), 583 nm ( $\log \epsilon=4.73$ ), 603 nm ( $\log \epsilon=4.70$ ) and 641 nm ( $\log \epsilon=4.61$ ) for compounds **1–4**, respectively; replacing the *tert*-butyl group in **2** by a phenyl group in **1** leads to a bathochromic shift of 41 nm; similarly, a bathochromic shift of 20 nm is observed when replacing the carboxymethyl substituent in **3** by the stronger electron-acceptor dicyanovinyl group (**1**); finally, the introduction of the electron donor hexyloxy moiety at the TPA (**4**) leads to a bathochromic shift of 17 nm respect to **1**. On the other hand, compounds **5–6** (Table 1, Figure S17) display a bathochromic shift respect to **1–4**, explained by the more extended conjugation due to the presence of the thiophene ring. In fact, **5** and **6** show light absorption through the whole visible region, including the near-IR, with maxima at 656 nm ( $\log \epsilon=4.83$ ) and 705 nm ( $\log \epsilon=4.51$ ), respectively. It is interesting to note that the absorption of **6** expands up to 900 nm, facilitating the absorption in this region of the solar emission. Utilization of materials that absorb light extending into the IR range is one of the strategies to increase solar light harvesting, thereby increasing power-efficiency.<sup>17</sup> The high molar extinction coefficient absorption bands are as well positive for light harvesting and hence photocurrent generation. In all cases, the intense absorption band can be attributed to the ICT from the TPA moiety (acting as donor) to the methylene substituted thiazole ring (acting as acceptor), behaviour that is already observed in related push–pull compounds.<sup>12a,18,19</sup>

Fluorescence Emission spectroscopy was employed to get information on the excited state–solvent interactions (Figure S18) and the results are reported in Table 1. The emission maxima are above 700 nm for compounds **1–4**, 800 nm for **5**, and above 900 nm for **6**. The large Stokes shift observed for compounds **1–5** (between 116 and 158 nm) can be attributed to the significant structural reorganization upon photoexcitation or to the charge transfer nature of the excited state.

To gain more detailed information on the push–pull character of these series of compounds, the UV–vis Absorption spectra of compounds **1**, **5** and **6** have been recorded in a series of solvents, presenting a large variation of polarity (THF, diethyl ether and dichloromethane) and Kamlet–Taft  $\pi^*$  constants.<sup>20</sup>

For all studied compounds, a positive solvatochromism, up to 42 nm for **1**, 31 nm for **5** and 35 nm for **6** (Figures S19), is observed by increasing the solvent polarity (Table S1), confirming the CT character of this band; moreover, we found an excellent correlation (correlation coefficient  $>0.99$ ) of the absorption maxima with the Kamlet–Taft  $\pi^*$  constants of the solvent (Table S2). The slope ( $S$ ) of the Kamlet–Taft equation ( $E=E_0+S\pi^*$ ), indicative of the solvatochromic sensibility, is higher for **1** ( $S=6.01$ ) than for **5** ( $S=3.91$ ) and **6** ( $S=3.89$ ) (Fig. 1, Table S2) indicating a higher polarizability of

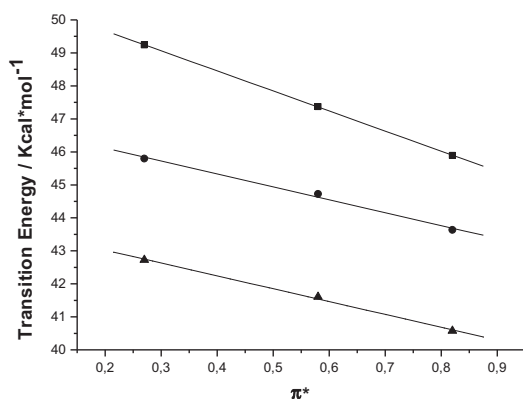


Fig. 1. Transition Energy of the low energy band for dyes **1** (square), **5** (circle) and **6** (triangle) versus Taft constant of solvents.

**1** and, consequently, better conjugation between the TPA moiety and the 2,2-dicyano-methylenethiazole acceptor unit.

The redox properties of **1–6** were investigated by CV and OSWV in ODCB–acetonitrile (5:1) and the potentials were recalculated over the value of the potential of  $F_c/F_c^+$  (0.08 V) using as reference (Table 1, Figures S20–S22). In the cathodic side, compounds **1–6** show a first reversible oxidation wave assigned to the TPA moiety based on the oxidation potential of TPA–CHO. A second non-reversible oxidation wave is observed at 0.96 V for **5**. A second and a third non-reversible oxidation waves were observed for **4** (0.88 V and 1.39 V) and **6** (0.76 V and 1.10 V). On the reduction side, compounds show an irreversible wave, probably due to the methylenethiazol moiety. The  $E_{HOMO}$  values were calculated with respect to ferrocene (Fc) as reference ( $E_{HOMO}$ :  $-5.1$  eV). Low-lying HOMO levels enable high open-circuit voltages and are, therefore, desirable.<sup>21</sup> The data shown in Table 1 indicate that the largest difference in the  $E_{HOMO}$  values, mostly depending on the TPA donor unit, occurs between compounds **2** and **6**, while the largest differences in the  $E_{LUMO}$  values occur between compounds **2** and **5**. Although those dyes with stronger acceptor units exhibit low-lying LUMO levels,  $E_{LUMO}$  of the dyes is still higher than that  $E_{LUMO}$  of PCBM ( $-4.3$  eV). Hence, the energetics of these dyes match quite well with PCBM to minimize energy waste upon electron transfer from the donor dye to the fullerene acceptor.

### 2.3. Theoretical calculations

The ground state geometry and the electron density distributions of HOMO and LUMO have been calculated using DFT at the B3LYP 6-31G\* (d, p) level in gas phase with Gaussian 03W. All the calculated distances and angles are in concordance with those determined by X-ray diffraction for analogous phenylthiazol-2-ylidene malononitrile systems.<sup>12a</sup> Fig. 2 shows the optimized structure of compound **4** to exemplify a typical conformation. The optimized structure of compounds **1–6** confirm that, in all cases, the D– $\pi$ –A system is essentially coplanar, being the dihedral angles between the corresponding electron donor fragment and the thiazole ring  $\approx 10^\circ$ . For the 4-phenylthiazole derivatives (**1**, **3–6**), the phenyl ring is twisted respect to the thiazole, with a calculated dihedral angle  $\sim 35^\circ$ , due to the substitution in 5-position of the thiazole ring, differently to the corresponding unsubstituted 4-phenylthiazole, which is coplanar.<sup>22</sup>

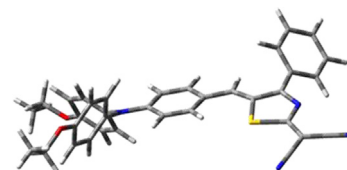


Fig. 2. Optimized geometry of compound **4**.

It is known that the substitution of the conjugated systems by terminal electron acceptors<sup>23</sup> causes that the aromatic character of the backbone changes to a partially quinoid-like character in which the degree of bond length alternation (BLA)<sup>24</sup> is significantly reduced. In our systems, the calculated BLA values (BLA=0.05 Å) reveals a partially quinoid character indicating the existence of intramolecular CT (ICT). As an example, in compound **6** the length of double bond between the electron acceptor fragment and the thiazole ring (1.385 Å) is significantly longer than the corresponding bond of the TCNQ (1.373 Å).<sup>25</sup> This fact suggests some zwitterionic contribution to the ground state.

The low-lying calculated HOMO levels of compounds **1–6** ( $-5.03$  to  $-5.44$  eV vs vacuum) are localized through the  $\pi$ -

conjugated system with an important contribution of the TPAs fragment. Nevertheless both orbitals, HOMO and LUMO (Fig. 3) are overlapped, favouring the HOMO to LUMO electronic transitions and so, increasing the double bond character of the single bonds (vide supra). The theoretical HOMO–LUMO gap is smaller for compounds **5** and **6** than those found for the series **1–4**, in agreement with the experimental values (Fig. 4).

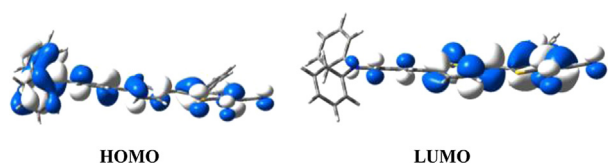


Fig. 3. Distribution of orbital coefficients of HOMO and LUMO of compound **5**.

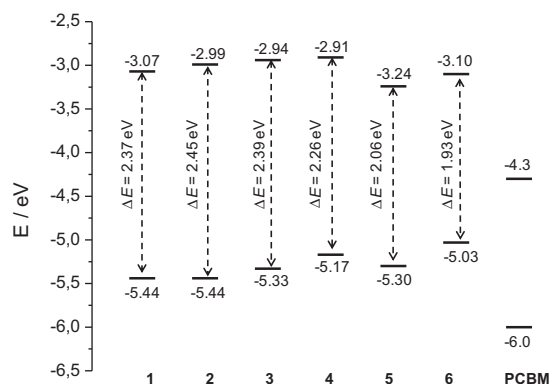


Fig. 4. HOMO–LUMO levels and band gap of compounds **1–6** and their relative position respecting PCBM.

In a photovoltaic cell,  $V_{OC}$  is proportional to the difference between the HOMO of the donor and the LUMO of the acceptor.<sup>21b</sup> In compounds **1–6**, the difference between the HOMO level of the dyes and the LUMO level of PCBM (–4.3 eV) are in the range of 1.41–0.73 eV, values, which should enable high open-circuit voltages. The LUMO levels vary by only 0.33 eV, being in the range –2.91 to –3.24 eV, higher than that of PCBM, in agreement to the electrochemically determined values.

#### 2.4. Preparation and characterization of SMOSC

The configuration of the device is shown in Fig. 5.

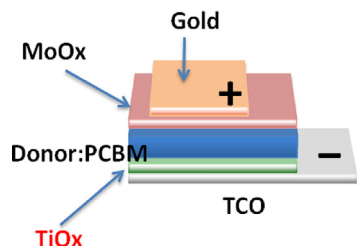


Fig. 5. Device configuration for dye/PCBM bulk heterojunction solar cells. MoO<sub>x</sub> and TiO<sub>x</sub> act as electron and hole blocking layer, respectively. TCO stands for a transparent conductive oxide acting as electrodes.

In the cell configuration used here the surface of transparent conducting electrode (TCO) is coated with a nanometric film of TiO<sub>x</sub> that should act as hole blocking layer.<sup>26</sup> The photoactive part of the device consists in a blend of the push–pull molecule acting as chromophore and electron donor molecule and PCBM as electron

acceptor in the photoinduced charge separation process. The device is completed by a gold cathode that was coated also with a thin layer of molybdenum oxide as electron blocking layer.<sup>27</sup> The performance of the SMOSCs was optimised with respect to the dye to PCBM proportion, and also with respect to the thickness of the TiO<sub>x</sub> and MoO<sub>x</sub> layers.

In a related precedent reporting the activity of solar cells for a series of merocyanine colorants in combination with PCBM, it was observed that the proportion between the chromophore and the PCBM plays an important role determining the current density and the overall efficiency of the cell.<sup>28</sup> It was concluded that in that case the maximum efficiency is achieved for PCBM weight percentages ranging from 65 to 85 % and there was a significant drop in current density in the regions below or above these proportions. In our case, we also proceeded to optimize this proportion between the dye and PCBM for compounds **1** and **4**. Aimed at this optimization a series of SMOSCs, prepared exactly under the same parameters and conditions, but in which the PCBM content was varied in the range of 70–90 %, were characterised. The results obtained indicate that the most appropriate proportion for maximum efficiency has a PCBM percentage about 80 %, a value, that is, close to that previously established for merocyanine dyes.<sup>29</sup> Fig. 6 shows some efficiency values indicating that 80 wt % is about the optimal dye/PCBM proportion for dyes **3** and **4**.

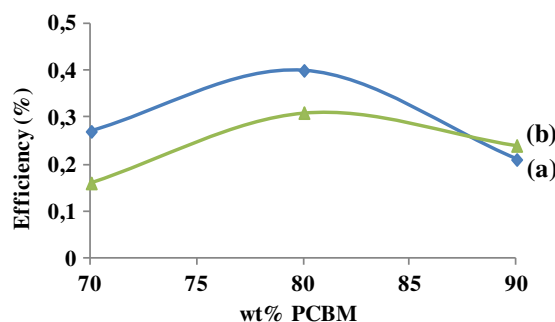


Fig. 6. Optimization of dye/PCBM ratio for compounds **3** (a) and **4** (b).

The existence of an optimal PCBM proportion with respect to the dye could be correlated with the quantum yield of the charge separation step and the need of an efficient quenching of the excited state of the dye by PCBM. This efficient quenching leading to charge separation may require a high PCBM content to minimise other decay pathways of the dye excited state alternative to charge separation.

After having optimised the composition of the photoactive layer, we proceeded to optimise the thickness of the dye/PCBM active layer as well as those of the hole and electron blocking layers. Plots of efficiency versus the thickness of these three layers are presented in Figs. 7 and 8. In the case of the donor–PCBM layer chlorobenzene

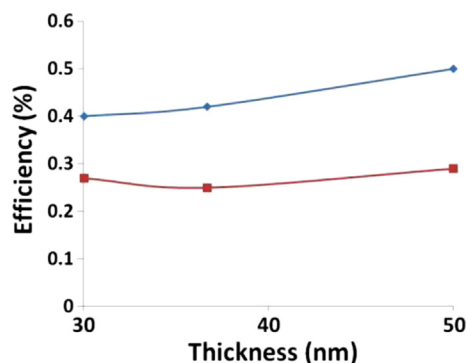
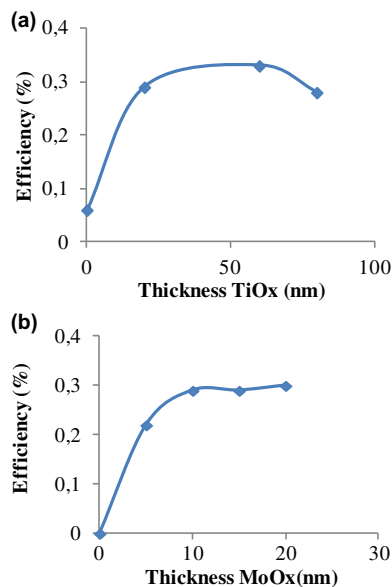


Fig. 7. Optimization of the dye/PCBM layer thickness for dyes **3** (a) and **4** (b).



**Fig. 8.** (a) Optimization of the hole blocking layer thickness. (b) Electron blocking layer thickness.

solutions of a mix of dye and PCBM in a proportion 20:80 wt % were cast by spin coating into TCO coated with  $\text{TiO}_x$  at different speeds and the resulting thickness determined by optical profilometry. It was established that the optimal thickness of the photoactive layer should be around 50 nm.

Concerning the  $\text{TiO}_x$  thickness in the range 0–80 nm it was observed that there is a region between 20 and 60 nm where the performance of the cell is the maximum, decreasing if the thickness is thinner or thicker than these values (Fig. 8a). Similar trend was observed for the thickness of the  $\text{MoO}_x$  layer and also from this study a suitable thickness for this electron blocking layer was selected (Fig. 8b).

After having optimized some parameters of the SMOSC for some selected dyes, we proceeded to the preparation under these conditions of photovoltaic devices for all the dyes **1–6** under study with the aim of obtaining data of the relative performance of the corresponding solar cells in order to establish a valid comparison of efficiency depending on the chemical structure of the dye. A summary of the results obtained is collected in Table 2.

**Table 2**  
Performance of TPA-based SMOSCs using compounds **1–6** as dyes and electron donor moieties

Compound	$J_{SC}$ (mA/cm <sup>2</sup> )	$V_{OC}$ (mV)	Fill factor (%)	Efficiency (%)
<b>1</b>	1.16	695.00	30.31	0.25
<b>2</b>	1.59	813.27	35.47	0.46
<b>3</b>	2.12	805.99	30.08	0.51
<b>4</b>	1.62	632.55	32.08	0.33
<b>5</b>	1.55	822.56	30.32	0.39
<b>6</b>	0.87	739.10	27.94	0.18
Two stacked cells (dye <b>3</b> )	1.75	1407	29.17	0.72
Three stacked cells (dye <b>3</b> )	1.54	2016	29.28	0.91

As it can be seen in this Table 3 although the theoretical  $V_{OC}$  values are higher than the experimental ones, as expected, the relative order predicted by theoretical calculations agrees reasonably well with the experimental  $V_{OC}$  values except for compounds **5** and **6**.

**Table 3**  
Comparison of energetic levels and open-circuit voltage for compounds **1–6**

Compound	$E_{HOMO}$ (eV) <sup>a</sup>	$V_{OC}^{teo}$ (mV) <sup>b</sup>	$V_{OC}^{exp}$ (mV)
<b>1</b>	−5.60	1000	695.00
<b>2</b>	−5.77	1170	813.27
<b>3</b>	−5.70	1100	805.99
<b>4</b>	−5.57	970	632.55
<b>5</b>	−5.61	1010	822.56
<b>6</b>	−5.37	770	739.10

<sup>a</sup> Calculated from  $E_{OX}$  measurements calibrated against Ferrocene/Ferrocenium ( $\text{Fc}/\text{Fc}^+$ ) redox couple (−5.1 eV).

<sup>b</sup> Theoretical  $V_{OC}$  calculated using the formula  $V_{OC} = (1/e)(E_{LUMOPCBM} - E_{HOMO}^{Donor} - 0.3 \text{ V})$ , where  $E_{LUMOPCBM} = -4.3 \text{ V}^{30}$  and  $E_{HOMO}^{Donor} = E_{HOMO}$  obtained by CV.

Overall a comparison of the data presented in Table 2 with those reported in the literature indicates that the efficiency of the cells prepared with the dyes **1–6** is mostly limited by the low current density at short circuit ( $J_{SC}$ ) measured for our cells.

In contrast, the  $V_{OC}$  values measured in our cells are in agreement with the expected energy levels of the HOMO (Dye) LUMO (PCBM) involved in the process and they are similar or even higher than those reported in the literature for organic solar cells.<sup>31</sup> Also the fill factor for our devices is not significantly lower than the reported values.<sup>32</sup> Therefore, from the performance data it can be concluded that the limiting factor of the efficiency of our cells is the low  $J_{SC}$  current.

The main reason of the low density current is probably the lack of complete light absorption due to the transparency of the cells. Fig. 9 shows a photograph of the solar cells prepared with dye **1** in which it can be seen that the cell is visually transparent. The transparency of the cell was quantitatively assessed by quantitative transmission optical spectroscopy that shows that the prepared cells with these dyes exhibit a low absorbance. In fact when the photoresponse of the cells in terms of incident photon-to-current conversion efficiency (IPCE) versus wavelength (Fig. 10) is corrected by the absorbance of the cell or light-harvesting efficiency (LHE) giving the absorbed photon-to-current conversion efficiency (APCE), a better understanding of the reasons of the efficiency data is obtained. These corrected photoresponses of some representative cells are also shown in Fig. 10. These APCE curves revealed high photon to electron conversion in a large range of wavelengths, indicating that the dyes exhibit a high efficiency in the conversion of light into current, similar or higher to those in the state of the art for SMOSC. According to these plots one of the main limitations of the dyes is the need to increase light harvesting, for instance, through an adequate engineering of the cell to increase sufficiently the thickness of the photoactive layer. However we have already commented that an increase of the thickness of the donor-PCBM layers has a negative influence derived from the higher charge recombination rate within the layer. Other factors like phase segregation with insufficient blending of the dyes with PCBM or the energy offset of chromophore LUMO to the LUMO of PCBM must also be considered and optimized in order to improve the efficiency of the SMOSC.

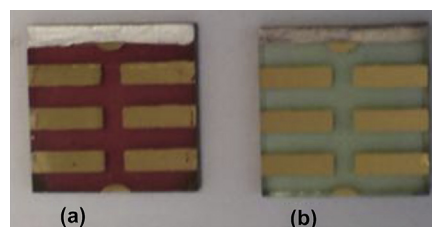


**Fig. 9.** (a) Photographs of conventional P3HT:PCBM devices. (b) Dye **1**: PCBM. The purpose is to provide a visual observation of the transparency of SMOSC prepared with dye **1**.

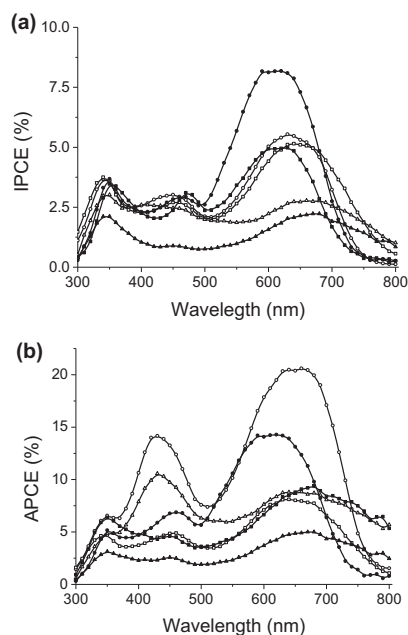


**Fig. 10.** (a) Photoresponse spectra plotted as incident photon-to-current conversion efficiency (IPCE). (b) APCE measured for SMOSCs based as dyes **1–6** as photosensitizers and electron donors and PCBM. Note the significant higher values of the efficiency in plot b.  $\Delta$ : dye **1**,  $\blacksquare$ : dye **2**,  $\bullet$ : dye **3**,  $\square$ : dye **4**,  $\circ$ : dye **5** and  $\blacktriangle$ : dye **6**.

In an attempt to optimise the performance of the SMOSCs by increasing photoabsorption we performed measurements in which a series of transparent cells were collated and connected in such a way that the combined response of two or three individual SMOSCs was determined. Under these conditions we have been able to increase the overall efficiency up to 0.91%, see Table 2 for two and three stacked cells connected electrically.

### 3. Experimental section

#### 3.1. Synthesis

**3.1.1. General synthetic procedures.** Synthetic procedures were carried out under inert argon atmosphere, in dry solvent unless otherwise noted. All reagents and solvents were reagent grade and were used without further purification. Chromatographic purifications were performed using silica gel 60 SDS (particle size 0.040–0.063 mm). Analytical thin-layer chromatography was performed using Merck TLC silica gel 60 F254.  $^1\text{H}$  NMR spectra were obtained on Bruker TopSpin AV-400 (400 MHz) spectrometer. Chemical shifts are reported in parts per million (ppm) relative to the solvent residual peak ( $\text{CDCl}_3$ , 7.27 ppm).  $^{13}\text{C}$  NMR chemical shifts ( $\delta$ ) are reported relative to the solvent residual peak ( $\text{CDCl}_3$ , 77.0 ppm). UV–vis measurements were carried out on a Shimadzu UV 3600 spectrophotometer. For extinction coefficient determination, solutions of different concentration were prepared in  $\text{CH}_2\text{Cl}_2$  (HPLC grade) with absorption between 0.1 and 1 of absorbance using a 1 cm UV cuvette. The emission measurements were carried out on Cary Eclipse fluorescence spectrophotometer. Mass spectra (MALDI-TOF) were recorded on a VOYAGER DE<sup>TM</sup> STR mass spectrometer using dithranol as matrix. Melting points are uncorrected.

Cyclic voltammetry was performed in ODCB–acetonitrile (5:1) solutions. Tetrabutylammonium perchlorate (0.1 M as supporting electrolyte) were purchased from Acros and used without purification. Solutions were deoxygenated by argon bubbling prior to

each experiment, which was run under argon atmosphere. Experiments were done in a one-compartment cell equipped with a platinum working microelectrode ( $\varnothing=2$  mm) and a platinum wire counter electrode. An  $\text{Ag}/\text{AgNO}_3$  (0.01 M in  $\text{CH}_3\text{CN}$ ) electrode was used as reference and checked against the  $F_c/F_c^+$  before and after each experiment.

The thermal stability was evaluated by TGA on Mettler Toledo TGA/DSC Start<sup>c</sup> System under nitrogen, with a heating rate of  $10^\circ\text{C}/\text{min}$ . Heating of crystalline samples leads to melting of the solids, but no recrystallization was observed.

Compounds 4-(diphenylamino)benzaldehyde (**7**), 5-formylthiophene-2-yl-2-boronic acid and 4-bromo-*N,N*-bis(phenyl)aniline (**12**) are commercially available and were used without further purification.

Compounds **8**,<sup>15</sup> **9**,<sup>7,12a</sup> **10**,<sup>7,13</sup> **11**,<sup>7</sup> **13**<sup>17</sup> and **14**<sup>16</sup> were synthesized according to literature procedures.

**3.1.2. General procedure for the synthesis of 14 and 15.** To a solution of corresponding bromide (1 mmol) and  $\text{PdCl}_2(\text{dppf})$  (0.1 mmol) in dry toluene (8 mL/mmol) was added a solution of 5-formylthiophene-2-yl-2-boronic acid (2 mmol) and  $\text{K}_2\text{CO}_3$  (5 mmol) in dry methanol (8 mL/mmol). The mixture was refluxed for 18 h. The reaction was quenched by the addition of water (20 mL) and extracted with  $\text{CH}_2\text{Cl}_2$  ( $3 \times 25$  mL). The combined organic extract was dried over anhydrous  $\text{MgSO}_4$  and filtered. Solvent was removed by rotary evaporation. The product was purified by column chromatography (silica gel, hexane– $\text{CHCl}_3$ , 1:1).

**3.1.2.1. 5-((4-(Diphenylamino)phenyl)thiophene-2-carbaldehyde (14).** 1.00 g of 4-Bromo-*N,N*-bis(phenyl)aniline (**12**) (3.1 mmol) and 966 mg of 5-formylthiophene-2-yl-2-boronic acid (6.20 mmol) were reacted according to the general procedure giving 846 mg of **14** as yellow oil (77% yield).  $^1\text{H}$  NMR (400 MHz,  $\text{CDCl}_3$ )  $\delta$ /ppm: 10.0 (s, 1H), 7.70 (d, 1H,  $J=4.0$  Hz), 7.50 (m, 2H), 7.30 (d, 1H,  $J=4.0$  Hz), 7.25 (m, 4H), 7.11 (m, 4H), 7.06 (m, 2H), 7.04 (m, 2H).  $^{13}\text{C}$  NMR (100 MHz,  $\text{CDCl}_3$ )  $\delta$ /ppm: 182.7, 154.6, 149.1, 147.0, 141.3, 137.8, 135.2, 129.5, 127.3, 126.1, 125.2, 125.0, 123.9, 122.9, 122.4. MS ( $m/z$ ) (MALDI-TOF): calculated  $\text{C}_{23}\text{H}_{17}\text{NOS}$ : 355.10; found ( $\text{M}+\text{H}^+$ ): 355.20, 356.20, 357.20.

**3.1.2.2. 5-((4-(Bis(4-hexyloxy)phenyl)amino)phenyl)thiophene-2-carbaldehyde (15).** 1.00 g of 4-Bromo-*N,N*-bis(4-(hexyloxy)phenyl)aniline (**13**) (1.91 mmol) and 595 mg of 5-formylthiophene-2-yl-2-boronic acid (3.82 mmol) were reacted according to the general procedure giving 795 mg of **15** as yellow oil (75% yield).  $^1\text{H}$  NMR (400 MHz,  $\text{CDCl}_3$ )  $\delta$ /ppm: 9.84 (s, 1H), 7.70 (d, 1H,  $J=4.0$  Hz), 7.46 (m, 2H), 7.26 (d, 1H,  $J=4.0$  Hz), 7.09 (m, 4H), 6.90 (m, 2H), 6.85 (m, 4H), 3.95 (t, 4H,  $J=6.5$  Hz), 1.52–1.42 (m, 4H), 1.40–1.32 (m, 8H), 0.92 (t, 6H,  $J=7.0$  Hz).  $^{13}\text{C}$  NMR (100 MHz,  $\text{CDCl}_3$ )  $\delta$ /ppm: 182.5, 156.1, 155.2, 150.0, 140.7, 139.7, 137.9, 127.2, 127.1, 124.0, 122.2, 119.2, 115.4, 68.2, 31.6, 29.3, 25.7, 22.6, 14.0. MS ( $m/z$ ) (MALDI-TOF): calculated  $\text{C}_{35}\text{H}_{41}\text{NO}_3\text{S}$ : 555.28; found ( $\text{M}+\text{H}^+$ ): 555.37, 556.34, 557.37.

**3.1.3. 2-(5-(4-(Diphenylamino)benzylidene)-4-phenylthiazol-2-(5H)-ylidene)malonitrile (1).** To a solution of 4-(diphenylamino)benzaldehyde (**7**) (Aldrich, 97%) (333 mg, 1.20 mmol) in 1.7 mL of acetic anhydride (1.5 mL/mmol) and 11 mL of ODCB (10 mL/mmol) under argon atmosphere was added to a stirred solution of 2-(4-phenylthiazol-2-yl)malonitrile (**9**) (250 mg, 1.11 mmol). The mixture was stirred at  $140^\circ\text{C}$  for 6 h. After cooling to room temperature, the reaction was extracted with diethyl ether, and the organic layer was dried over  $\text{MgSO}_4$  (anhydrous). After filtration of the drying agent, the solvent was removed under vacuum. Compound **1** was purified by column chromatography (silica gel, hexane–ethyl acetate, 7:3). The final product **1** was recrystallized in  $\text{CH}_2\text{Cl}_2$ –hexane as blue solid with 60% yield (320 mg). Mp:  $>300$

with decomposition.  $^1\text{H}$  NMR (400 MHz,  $\text{CDCl}_3$ )  $\delta$ /ppm: 7.80 (m, 2H), 7.66 (m, 1H), 7.60 (s, 1H), 7.58 (m, 2H), 7.48 (m, 2H), 7.4 (m, 4H), 7.25 (m, 2H), 7.22 (m, 4H), 7.03 (m, 2H).  $^{13}\text{C}$  NMR (100 MHz,  $\text{CDCl}_3$ )  $\delta$ /ppm: 182.4, 180.6, 152.3, 145.2, 141.6, 133.6, 132.3, 132.0, 131.7, 130.5, 130.0, 129.0, 162.6, 126.1, 125.0, 119.4, 115.1, 113.2, 65.7. UV–vis ( $\text{CH}_2\text{Cl}_2$ )  $\lambda_{\text{max}}$ /nm (log  $\epsilon$ ): 624 (4.7), 425.0 (4.0), 339 (4.2). IR  $\nu/\text{cm}^{-1}$ : 3061, 2925, 2210, 1590, 1562, 1495, 1422, 1335, 1299, 1177, 1096, 700. MS ( $m/z$ ) (MALDI-TOF): calculated  $\text{C}_{31}\text{H}_{20}\text{N}_4\text{S}$ : 480.14; found ( $\text{M}+\text{H}^+$ ): 480.2, 481.20, 482.2, 483.2, 484.2.

**3.1.4. 2-(5-(4-(Diphenylamino)benzylidene)-4-tert-butylthiazol-2(5H)-ylidene)malonitrile (2).** A solution of 4-(diphenylamino)benzaldehyde (**7**) (423 mg, 1.55 mmol) in 1.0 mL of acetic anhydride (1.5 mL/mmol) was added under argon atmosphere to a stirred solution of 2-(4-tert-butylthiazol-2-yl)malononitrile (**10**) (200 mg, 0.77 mmol). The mixture was stirred at 140 °C for 2 h. After cooling to room temperature, the reaction was extracted with diethyl ether, and the organic layer was dried over  $\text{MgSO}_4$  (anhydrous). After filtration of the drying agent, the solvent was removed under vacuum. Compound **2** was purified by column chromatography (silica gel, hexane–ethyl acetate, 7:3). The final product **2** was recrystallized in  $\text{CH}_2\text{Cl}_2$ –hexane as blue solid with 65% yield (260 mg).  $^1\text{H}$  NMR (400 MHz,  $\text{CDCl}_3$ )  $\delta$ /ppm: 7.89 (s, 1H), 7.49 (m, 2H), 7.38 (m, 4H), 7.23 (m, 2H), 7.21 (m, 4H), 7.05 (m, 2H), 1.58 (d, 9H).  $^{13}\text{C}$  NMR (100 MHz,  $\text{CDCl}_3$ )  $\delta$ /ppm: 190.8, 181.9, 151.6, 145.4, 137.7, 133.1, 130.9, 129.9, 126.4, 125.7, 124.7, 119.7, 114.8, 112.9, 66.6, 38.9, 31.2. Mp: 347–350 °C. UV–vis ( $\text{CH}_2\text{Cl}_2$ )  $\lambda_{\text{max}}$ /nm (log  $\epsilon$ ): 683 (4.7), 405 (3.9), 298 (4.3). IR  $\nu/\text{cm}^{-1}$ : 3055, 2971, 2214, 1610, 1592, 1566, 1507, 1448, 1433, 1335, 1302, 1197, 1174, 1137, 699. MS ( $m/z$ ) (MALDI-TOF): calculated  $\text{C}_{29}\text{H}_{24}\text{N}_4\text{S}$ : 460.17; found ( $\text{M}+\text{H}^+$ ): 460.20, 461.3, 462.3, 463.3.

**3.1.5. Methyl 2-cyano-2-(5-(4-(diphenylamino)benzylidene)-4-phenylthiazol-2(5H)-ylidene)acetate (3).** A solution of 4-(diphenylamino)benzaldehyde (**7**) (366 mg, 1.34 mmol) in 1.8 mL of acetic anhydride (1.5 mL/mmol) and 12.0 mL of ODCB (1.5 mL/mmol) under argon atmosphere was added to a stirred solution of methyl cyano(4-phenyl-1,3-thiazol-2-yl)acetate (**11**) (250 mg, 1.22 mmol). The mixture was stirred at 140 °C for 2 h. After cooling to room temperature, the reaction was extracted with diethyl ether, and the organic layer was dried over  $\text{MgSO}_4$  (anhydrous). After filtration of the drying agent, the solvent was removed under vacuum. Compound **3** was purified by column chromatography (silica gel, hexane–ethyl acetate, 7:3). The final product **3** was recrystallized in  $\text{CH}_2\text{Cl}_2$ –pentane as blue solid with 52% yield (292 mg). Mp: >300 with decomposition.  $^1\text{H}$  NMR (400 MHz,  $\text{CDCl}_3$ )  $\delta$ /ppm: 7.82 (m, 2H), 7.62 (mt, 1H,  $J=2.3$  Hz), 7.359–7.53 (m, 5H), 7.38 (md, 4H,  $J=1.7$  Hz), 7.23 (m, 2H), 7.19 (m, 4H), 7.02 (m, 2H), 3.92 (s, 3H).  $^{13}\text{C}$  NMR (100 MHz,  $\text{CDCl}_3$ )  $\delta$ /ppm: 179.6, 179.6, 166.2, 151.5, 145.5, 140.9, 134.1, 133.5, 132.3, 131.7, 130.5, 129.8, 128.8, 126.4, 125.9, 125.6, 119.7, 116.0, 87.1, 52.7. UV–vis ( $\text{CH}_2\text{Cl}_2$ )  $\lambda_{\text{max}}$ /nm (log  $\epsilon$ ): 603 (4.7), 582 (4.7), 417 (3.9), 332 (4.1), 286 (4.3). IR  $\nu/\text{cm}^{-1}$ : 3059, 3029, 2943, 2214, 1700, 1564, 1489, 1462, 1280, 1191, 1175, 1079, 701. MS ( $m/z$ ) (MALDI-TOF): calculated  $\text{C}_{32}\text{H}_{23}\text{N}_3\text{O}_2\text{S}$ : 513.15; found ( $\text{M}+\text{H}^+$ ): 513.2, 514.2, 515.2, 516.2, 517.2.

**3.1.6. 2-(5-(4-(Bis(4-(hexyloxy)phenylamino)benzylidene)-4-phenylthiazol-2(5H)-ylidene)malonitrile (4).** A solution of 4-bis(4-(hexyloxy)phenylamino)benzaldehyde (**8**) (60 mg, 1.22 mmol) in 1.6 mL of acetic anhydride (1.5 mL/mmol) and 11 mL ODCB (10 mL/mmol) under argon atmosphere was added to a stirred solution of 2-(4-phenylthiazol-2-yl)malononitrile (**9**) (250 mg, 1.11 mmol) in acetic anhydride under argon atmosphere. The mixture was stirred at 140 °C for 6 h. After cooling to room temperature, the reaction was extracted with diethyl ether, and the organic layer was dried

over  $\text{MgSO}_4$  (anhydrous). After filtration of the drying agent, the solvent was removed under vacuum. Compound **4** was purified by column chromatography (silica gel, hexane–ethyl acetate, 7:3). The final product **4** was recrystallized in  $\text{CH}_2\text{Cl}_2$ –pentane as blue solid with 42% yield (317 mg). Mp: >300 with decomposition.  $^1\text{H}$  NMR (400 MHz,  $\text{CDCl}_3$ )  $\delta$ /ppm: 7.78 (m, 2H), 7.63 (mt, 1H,  $J=2.10$  Hz), 7.57 (m, 3H), 7.44 (m, 2H), 7.13 (m, 4H), 6.91 (m, 4H), 6.89 (m, 2H), 3.96 (t, 4H,  $J=6.6$  Hz), 6.89 (d, 2H,  $J=9.0$  Hz), 3.96 (t, 4H,  $J=6.6$  Hz), 1.8 (dt, 4H,  $J=14.8, 6.6$  Hz), 1.47 (m, 4H), 1.38–1.32 (m, 8H), 0.92 (t, 6H,  $J=7.0$  Hz).  $^{13}\text{C}$  NMR (100 MHz,  $\text{CDCl}_3$ )  $\delta$ /ppm: 182.4, 180.2, 157.5, 153.1, 141.9, 137.5, 134.0, 132.0, 131.9, 131.0, 130.5, 128.9, 128.0, 123.7, 117.5, 115.5, 115.4, 113.5, 68.4, 31.5, 29.2, 27.7, 22.6, 14.0. UV–vis ( $\text{CH}_2\text{Cl}_2$ )  $\lambda_{\text{max}}$ /nm (log  $\epsilon$ ): 641 (4.6), 431 (3.8), 334 (4.1). IR  $\nu/\text{cm}^{-1}$ : 2950, 2929, 2857, 2207, 1501, 1449, 1421, 1333, 1234, 1178, 1157, 1094. MS ( $m/z$ ) (MALDI-TOF): calculated  $\text{C}_{43}\text{H}_{44}\text{N}_4\text{O}_2\text{S}$ : 680.32; found ( $\text{M}+\text{H}^+$ ): 680.4, 681.4, 682.4, 683.4, 684.4.

**3.1.7. 2-(5-(5-(4-(Diphenylamino)phenyl)thiophen-2-yl)methylene)-4-phenylthiazol-2(5H)-ylidene)malonitrile (5).** A solution of 5-(4-(diphenylamino)phenyl)thiophene-2-carbaldehyde (**14**) (433 mg, 1.22 mmol) in 1.7 mL of acetic anhydride (1.5 mL/mmol) and 11 mL ODCB (10 mL/mmol) under argon atmosphere was added to a stirred solution of 2-(4-phenylthiazol-2-yl)malononitrile (**9**) (250 mg, 1.11 mmol) in acetic anhydride under argon atmosphere. The mixture was stirred at 140 °C for 6 h. After cooling to room temperature, the reaction was extracted with diethyl ether, and the organic layer was dried over  $\text{MgSO}_4$  (anhydrous). After filtration of the drying agent, the solvent was removed under vacuum. Compound **5** was purified by column chromatography (silica gel, hexane–ethyl acetate, 7:3). The final product **5** was recrystallized in  $\text{CH}_2\text{Cl}_2$ –hexane as blue solid with 40% yield (249 mg). Mp: >300 with decomposition.  $^1\text{H}$  NMR (400 MHz,  $\text{CDCl}_3$ )  $\delta$ /ppm: 7.81 (m, 3H), 7.67 (m, 1H), 7.60 (m, 2H), 7.58 (m, 2H), 7.52 (m, 1H), 7.39 (m, 1H), 7.33 (m, 4H), 7.17 (m, 4H), 7.14 (m, 2H), 7.08 (m, 2H).  $^{13}\text{C}$  NMR (100 MHz,  $\text{CDCl}_3$ )  $\delta$ /ppm: 181.3, 179.7, 157.2, 149.9, 146.5, 139.7, 136.9, 132.8, 132.5, 131.4, 130.2, 129.6, 129.5, 129.1, 127.4, 125.5, 125.1, 124.4, 121.7, 115.0, 113.1, 66.5. UV–vis ( $\text{CH}_2\text{Cl}_2$ )  $\lambda_{\text{max}}$ /nm (log  $\epsilon$ ): 656 (4.8), 474 (4.3), 363 (4.5), 300 (4.5). IR  $\nu/\text{cm}^{-1}$ : 2924, 2852, 2212, 1559, 1488, 1408, 1326, 1287, 1188, 1092, 1069, 696. MS ( $m/z$ ) (MALDI-TOF): calculated  $\text{C}_{35}\text{H}_{22}\text{N}_4\text{S}_2$ : 562.13; found ( $\text{M}+\text{H}^+$ ): 562.2, 563.2, 564.2, 465.2, 565.2, 566.2.

**3.1.8. 2-(5-(5-(4-(Bis(4-(hexyloxy)phenyl)amino)phenyl)thiophen-2-yl)methylene)-4-phenylthiazol-2(5H)-ylidene)malonitrile (6).** A solution of 5-(4-(bis(hexyloxy)phenyl)amino)phenylthiophene-2-carbaldehyde (**15**) (677 mg, 1.22 mmol) in 1.7 mL of acetic anhydride (1.5 mL/mmol) and 11 mL ODCB (10 mL/mmol) under argon atmosphere was added to a stirred solution of 2-(4-phenylthiazol-2-yl)malononitrile (**9**) (250 mg, 1.11 mmol) in acetic anhydride under argon atmosphere. The mixture was stirred at 140 °C for 6 h. After cooling to room temperature, the reaction was extracted with diethyl ether, and the organic layer was dried over  $\text{MgSO}_4$  (anhydrous). After filtration of the drying agent, the solvent was removed under vacuum. Compound **6** was purified by column chromatography (silica gel, hexane–ethyl acetate, 7:3). The final product **6** was recrystallized in  $\text{CH}_2\text{Cl}_2$ –pentane as blue solid with 35% yield (295 mg). Mp: >300 with decomposition.  $^1\text{H}$  NMR (400 MHz,  $\text{CDCl}_3$ )  $\delta$ /ppm: 7.80 (m, 3H), 7.65 (m, 1H), 7.59 (mt, 2H,  $J=1.4$  Hz), 7.51 (m, 2H), 7.50 (d, 1H,  $J=4.2$  Hz), 7.34 (d, 1H,  $J=4.2$  Hz), 6.91 (m, 2H), 6.88 (m, 4H), 3.96 (t, 4H,  $J=6.6$  Hz), 1.80 (dt, 4H,  $J=15.0, 6.6$  Hz), 1.50 (m, 4H), 1.36 (m, 8H), 1.1 (t, 6H,  $J=7.0$  Hz).  $^{13}\text{C}$  NMR (100 MHz,  $\text{CDCl}_3$ )  $\delta$ /ppm: 181.3, 179.4, 158.1, 156.5, 140.0, 139.0, 136.4, 132.9, 131.6, 130.2, 129.1, 127.4, 123.2, 118.7, 115.4, 115.2, 113.3, 68.5, 67.8, 31.6, 29.2, 25.7, 22.6, 14.0. UV–vis ( $\text{CH}_2\text{Cl}_2$ )  $\lambda_{\text{max}}$ /nm (log  $\epsilon$ ): 705 (4.5), 494 (4.1), 372 (4.3), 294 (4.3). IR  $\nu/\text{cm}^{-1}$ : 2951, 2927, 2856, 2210, 1589, 1558, 1504, 1405, 1322, 1241, 1185, 1066, 825. MS ( $m/z$ )

(MALDI-TOF): calculated  $C_{47}H_{46}N_4O_2S_2$ : 762.31; found ( $M+H^+$ ): 762.4, 763.4, 765.4, 766.4, 767.4.

### 3.2. Preparation of SMOSCs

All samples were prepared on ITO-coated glass substrates with sheet resistance  $15 \Omega \text{ sq}^{-1}$  from Psiotec Ltd., which were first cleaned by ultrasonic agitation in acetone and isopropanol. Freshly cleaned substrate was then covered with a dense  $TiO_x$  layer using spin coating (50 nm).<sup>27</sup> Solutions of dye/PCBM were prepared at 20:80 wt % and 30 mg/mL in chlorobenzene and were deposited by spin coating on top of the  $TiO_x$  dense layer.  $MoO_x$  layer was deposited by thermal evaporation (20 nm) using  $MoO_2$  powder as precursor. Finally, a layer of gold was deposited by thermal evaporation (100 nm) using a shadow mask obtaining an active area pixel of  $0.048 \text{ cm}^2$ . The thickness of all of the films was measured by a MicroXAM-100 3D surface profilometer.

Stacked cells were prepared by stacking two or three single devices connected in series using conductive metallic paint.

### 3.3. Photovoltaic response measurements

To determine the  $J_{SC}-V_{OC}$  plots, the cell was connected to a sourceMeter (Keithley 2601). The voltage scan was controlled using ReRa Tracer software. The data were automatically transferred to a PC that controlled the experiment and at the same time provided data storage capability to the system. The solar simulator (Sun 2000, ABET Technologies) was equipped with an AM 1.5G filter and the nominal power for the measurements was  $100 \text{ mW/cm}^2$ . The same cells were used to record the IPCE spectra. In IPCE measurements the sample was excited with a 150 W xenon lamp through a Czerny–Turner monochromator. The current output at short circuit was measured by a potentiostat (AMEL), which transferred the data through the A/D converter to the PC controlling the monochromator apparatus. IPCE curves were calculated using a Newport (818-UV-L) calibrated photodiode.

## 4. Conclusions

The present work has shown that a series of push–pull chromophores containing TPA can exhibit moderate intrinsic efficiency as photoactive component in SMOSCs based on PCBM according to the absorbed photon to current efficiency. The limiting factor efficiency is the low photon absorption due to the transparency of the cell derived from the thinness of the photoactive layer. However, the positive effect of preparing thicker films is counter balanced by the negative effect of charge recombination due to the short free mean paths of the charge carrier. Other reasons for the low efficiency could be phase segregation of dye and PCBM or an inadequate match of the LUMO energy of the dye and PCBM. The efficiency can be somewhat improved by designing stacked devices constituted by two independent cells in series. Nevertheless, optimization of the design of the dyes by further increasing their molar absorption coefficient without modifying other parameters related to photovoltaic activity such as HOMO energy and photoinduced charge separation quantum yield is likely to be reflected in a higher efficiency of the cell. Further work in this direction is currently undertaken in our laboratory.

## Acknowledgements

Financial support from the Ministry of Science and Innovation of Spain (CTQ2010-17498, CTQ2012-32315, PLE2009-0038 and Consolider-Ingenio Projects HOPE CSD2007-00007 and MULTICAT) is gratefully acknowledged. P.A. also thanks the Spanish Ministry of Science and Innovation by a Juan de la Cierva research associate contract.

## Supplementary data

Supplementary data related to this article can be found at <http://dx.doi.org/10.1016/j.tet.2013.05.137>.

## References and notes

- (a) Brabec, C. J.; Sariciftci, N. S.; Hummelen, J. C. *Adv. Funct. Mater.* **2001**, *11*, 15–26; Sariciftci, N. S.; Günes, S.; Neugebauer, H. *Chem. Rev.* **2007**, *107*, 1324–1338; (b) Walzer, K.; Männig, B.; Pfeiffer, M.; Leo, K. *Chem. Rev.* **2007**, *107*, 1233–1271.
- (a) Cheng, Y.-J.; Yang, S.-H.; Hsu, C.-S. *Chem. Rev.* **2009**, *109*, 5868–5923; (b) Walker, B.; Kim, C.; Nguyen, T.-Q. *Chem. Mater.* **2011**, *23*, 470–482.
- Mishra, A.; Ma, C.-Q.; Bäuerle, P. *Chem. Rev.* **2009**, *109*, 1141–1276.
- (a) Lin, Y.; Li, Y.; Zhan, X. *Chem. Soc. Rev.* **2012**, *41*, 4245–4272; (b) Mishra, A.; Bäuerle, P. *Angew. Chem., Int. Ed.* **2012**, *51*, 2020–2067.
- <http://www.heliotech.com>.
- Steinberger, S.; Mishra, A.; Reinold, E.; Mena-Osteritz, E.; Müller, H.; Uhrich, C.; Pfeiffer, M.; Bäuerle, P. *J. Mater. Chem.* **2012**, *22*, 2701–2712.
- Bürckstümmer, H.; Tulyakova, E. V.; Deppisch, M.; Lenze, M. R.; Kronenberg, N. M.; Gsänger, M.; Stolte, M.; Meerholz, K.; Würthner, F. *Angew. Chem., Int. Ed.* **2011**, *50*, 11628–11632.
- (a) Demeter, D.; Jeux, V.; Leriche, P.; Blanchard, P.; Olivier, Y.; Cornil, J.; Po, R.; Roncali, J. *Adv. Funct. Mater.* **2013**, <http://dx.doi.org/10.1002/adfm.201300427>; (b) Jeux, V.; Demeter, D.; Leriche, P.; Roncali, J. *RSC Adv.* **2013**, *3*, 5811–5814.
- (a) Shirota, Y.; Kageyama, H. *Chem. Rev.* **2007**, *107*, 953–1010; (b) Ning, Z.; Tian, H. *Chem. Commun.* **2009**, 5483–5495.
- (a) Karpe, S.; Cravino, A.; Frere, P.; Allain, M.; Mabon, G.; Roncali, J. *Adv. Funct. Mater.* **2007**, *17*, 1163–1171; (b) Roquet, S.; Cravino, A.; Leriche, P.; Alevque, O.; Frere, P.; Roncali, J. *J. Am. Chem. Soc.* **2006**, *128*, 3459–3466; (c) Cravino, A.; Leriche, P.; Alevque, O.; Roquet, S.; Roncali, J. *Adv. Mater.* **2006**, *18*, 3033–3037; (d) Wu, G.; Zhao, G.; He, C.; Zhang, J.; He, Q.; Chen, X.; Li, Y. *Sol. Energy Mater. Sol. Cells* **2009**, *93*, 108–113; (e) Leriche, P.; Frere, P.; Cravino, A.; Alevque, O.; Roncali, J. *J. Org. Chem.* **2007**, *72*, 8332–8336.
- Würthner, F.; Yao, S.; Debaerdemaeker, T.; Wortmann, R. *J. Am. Chem. Soc.* **2002**, *124*, 9431–9447.
- (a) Andreu, R.; Galán, E.; Orduna, J.; Villacampa, B.; Alicante, R.; López Navarrete, J. T.; Casado, J.; Garín, J. *Chem.–Eur. J.* **2011**, *17*, 826–838; (b) Andreu, R.; Galán, E.; Garín, J.; Orduna, J.; Alicante, R.; Villacampa, B. *Tetrahedron Lett.* **2010**, *51*, 6863–6866; (c) Galán, E.; Andreu, R.; Garín, J.; Mosteo, L.; Orduna, J.; Villacampa, B.; Diosdado, B. E. *Tetrahedron* **2012**, *68*, 6427–6437.
- The synthesis of compound 3 was previously described by us: Gómez-Esteban, S.; de la Cruz, P.; Aljarilla, A.; Arellano, L. M.; Langa, F. *Org. Lett.* **2011**, *13*, 5362–5365.
- Nguyen, H. M.; Mane, R. S.; Ganesh, T.; Han, S. H.; Kim, N. J. *Phys. Chem. C* **2009**, *113*, 9206–9209.
- (a) Hagberg, D. P.; Marinado, T.; Karlsson, K. M.; Nonomura, K.; Qin, P.; Boschloo, G.; Brinck, T.; Hagfeldt, A.; Sun, L. J. *Org. Chem.* **2007**, *72*, 9550–9556; (b) Leliège, A.; Le Régent, C.-H.; Allain, M.; Blanchard, P.; Roncali, J. *Chem. Commun.* **2012**, *48*, 8907–8909.
- (a) Xu, M. F.; Li, R. Z.; Pootrakulchote, N.; Shi, D.; Guo, J.; Yi, Z. H.; Zakeeruddin, S. M.; Grätzel, M.; Wang, P. *J. Phys. Chem. C* **2008**, *112*, 19770–19776; (b) Aljarilla, A.; Lopez-Arroyo, L.; de la Cruz, P.; Oswald, F.; Meyer, T. B.; Langa, F. *Org. Lett.* **2012**, *14*, 5732–5735.
- (a) Langa, F.; de la Cruz, P.; Espíldora, E.; de la Hoz, A.; Bourdelande, J.; Sanchez, L.; Martin, N. J. *J. Org. Chem.* **2001**, *66*, 5033–5041; (b) Wang, X.; Perzon, E.; Delgado, J. L.; de la Cruz, P.; Zhang, F.; Langa, F.; Andersson, M. R.; Inganäs, O. *Appl. Phys. Lett.* **2004**, *85*, 5081–5083; (c) Wang, X.; Perzon, E.; Oswald, F.; Langa, F.; Admassie, S.; Andersson, M. R.; Inganäs, O. *Adv. Funct. Mater.* **2005**, *15*, 1665–1670; (d) Wang, X.; Perzon, E.; Oswald, F.; Langa, F.; Admassie, S.; Andersson, M. R.; Inganäs, O. *Adv. Funct. Mater.* **2005**, *15*, 1665–1670.
- (a) Beckmann, S.; Eitzbach, K.-H.; Krämer, P.; Lukaszuk, K.; Matschiner, R.; Schmidt, A. J.; Schuhmacher, P.; Sens, R.; Seybold, G.; Wortmann, R.; Würthner, F. *Adv. Mater.* **1999**, *11*, 536–541; (b) Spange, S.; Sens, R.; Zimmermann, Y.; Seifert, A.; Roth, I.; Anders, S.; Hofmann, K. *New J. Chem.* **2003**, *27*, 520–524.
- Würthner, F.; Archetti, G.; Schmidt, R.; Kuball, H. G. *Angew. Chem.* **2008**, *47*, 4529–4532.
- (a) Ripaud, E.; Olivier, Y.; Leriche, P.; Cornil, J.; Roncali, J. *J. Phys. Chem. B* **2011**, *115*, 9379–9386; (b) Kamlet, M. J.; Abboud, J. L.; Taft, R. W. *J. Am. Chem. Soc.* **1977**, *99*, 6027–6038; (c) Kamlet, M. J.; Abboud, J. L.; Abraham, M. H.; Taft, R. W. *J. Org. Chem.* **1983**, *48*, 2877–2887.
- (a) Cravino, A. *Appl. Phys. Lett.* **2007**, *91*, 243502–243504; (b) Dennler, G.; Scharber, M. C.; Brabec, C. J. *Adv. Mater.* **2009**, *21*, 1323–1338.
- (a) Au-Alvarez, O.; Peterson, R. C.; Crespo, A. A.; Esteva, Y. R.; Alvarez, H. M.; Stiven, A. M. P.; Hernández, R. P. *Acta Crystallogr., Sect. C* **1999**, *55*, 821–823; (b) Nesterov, V. N.; Montoya, N. G.; Yu, M.; Antipin, M.; Sanghadasa, M.; Clark, R. D.; Timofeeva, T. V. *Acta Crystallogr., Sect. C* **2002**, *58*, 72–75.
- Casado, J.; Pappenfus, T. M.; Miller, L. L.; Mann, K. R.; Ortí, E.; Viruela, P. M.; Pou-Américo, R.; Hernández, V.; López Navarrete, J. T. *J. Am. Chem. Soc.* **2003**, *125*, 2524–2534.
- (a) van Mullekom, H. A. M.; Vekemans, J. A. J. M.; Havinga, E. E.; Meijer, E. W. *Mater. Sci. Eng.* **2001**, *32*, 1–40; (b) Kertesz, M.; Choi, C. H.; Yang, S. *Chem. Rev.* **2005**, *105*, 3448–3481.
- Flandrois, S.; Chasseau, D. *Acta Crystallogr., Sect. B* **1977**, *33*, 2744–2750.

26. (a) Credgington, D.; Hamilton, R.; Atienzar, P.; Nelson, J.; Durrant, J. R. *Adv. Funct. Mater.* **2011**, *21*, 2744–2753; (b) Voigt, M. M.; Mackenzie, R. C. I.; Yau, C. P.; Atienzar, P.; Dane, J.; Keivanidis, P. E.; Bradley, D. D. C.; Nelson, J. *Sol. Energy Mater. Sol. Cells* **2011**, *95*, 731–734.
27. Sun, Y. M.; Takacs, C. J.; Cowan, S. R.; Seo, J. H.; Gong, X.; Roy, A.; Heeger, A. J. *Adv. Mater.* **2011**, *23*, 2226–2230.
28. (a) Hoppe, H.; Sariciftci, N. S. *J. Mater. Chem.* **2006**, *16*, 45–61; (b) Campoy-Quiles, M.; Ferenczi, T.; Agostinelli, T.; Etchegoin, P. G.; Kim, Y.; Anthopoulos, T. D.; Stavrinou, P. N.; Bradley, D. D. C.; Nelson, J. *Nat. Mater.* **2008**, *7*, 158–164.
29. Kronenberg, N. M.; Deppisch, M.; Wurthner, F.; Lademann, H. W. A.; Deing, K.; Meerholz, K. *Chem. Commun.* **2008**, 6489–6491.
30. Scharber, M. C.; Mühlbacher, D.; Koppe, M.; Denk, P.; Waldauf, C.; Heeger, A. J.; Brabec, C. J. *Adv. Mater.* **2006**, *18*, 789–794.
31. Sun, Y.; Welch, G. C.; Leong, W. L.; Takacs, C. J.; Bazan, G. C.; Heeger, A. J. *Nat. Mater.* **2012**, *11*, 44–48.
32. (a) Walker, B.; Tamayo, A. B.; Dang, X.-D.; Zalar, P.; Seo, J. H.; Garcia, A.; Tantiwivat, M.; Nguyen, T.-Q. *Adv. Funct. Mater.* **2009**, *19*, 3063–3069; (b) Lloyd, M. T.; Mayer, A. C.; Subramanian, S.; Mourey, D. A.; Herman, D. J.; Bapat, A. V.; Anthony, J. E.; Malliaras, G. G. *J. Am. Chem. Soc.* **2007**, *129*, 9144–9149.